Journal of Solid State Chemistry 182 (2009) 1319–1325

Contents lists available at ScienceDirect

Journal of Solid State Chemistry

journal homepage: www.elsevier.com/locate/jssc

Magnetic and structural properties of Na*Ln*MnWO$_6$ and Na*Ln*MgWO$_6$ perovskites

Graham King *, Lora M. Wayman, Patrick M. Woodward

The Ohio State University, Department of Chemistry, 100 West 18th Avenue, Columbus, OH 43210-1185, USA

ARTICLE INFO

Article history:
Received 20 December 2008
Received in revised form
16 February 2009
Accepted 25 February 2009
Available online 6 March 2009

Keywords:
Perovskites
A-site cation ordering
Powder X-ray diffraction
Structural trends
Magnetism

ABSTRACT

We have prepared 14 new *AA′BB′*O$_6$ perovskites which possess a rock salt ordering of the *B*-site cations and a layered ordering of the *A*-site cations. The compositions obtained are Na*Ln*MnWO$_6$ (*Ln* = Ce, Pr, Sm, Gd, Dy, and Ho) and Na*Ln*MgWO$_6$ (*Ln* = Ce, Pr, Sm, Eu, Gd, Tb, Dy, and Ho). The samples were structurally characterized by powder X-ray diffraction which has revealed metrically tetragonal lattice parameters for compositions with *Ln* = Ce, Pr and monoclinic symmetry for compositions with smaller lanthanides. Magnetic susceptibility vs. temperature measurements have found that all six Na*Ln*MnWO$_6$ compounds undergo antiferromagnetic ordering at temperatures between 10 and 13 K. Several compounds show signs of a second magnetic phase transition. One sample, NaPrMnWO$_6$, appears to pass through at least three magnetic phase transitions within a narrow temperature range. All eight Na*Ln*MgWO$_6$ compounds remain paramagnetic down to 2 K revealing that the ordering of the *Ln*$^{3+}$ cations in the Na*Ln*MnWO$_6$ compounds is induced by the ordering of the Mn^{2+} sub-lattice.

1. Introduction

Stoichiometric *AA′BB′*O$_6$ perovskites that have an ordering of both the *A*- and *B*-site cations have been the subject of several recent studies [1–4]. These compounds have been found to undergo a variety of different forms of complex ordering, both crystallographic and magnetic. Perovskites that have an ordering of both the cation sub-lattices are quite rare. While rock salt ordering of the *B*-site cations is common, perovskites with *A*-site cation ordering are uncommon. By making appropriate choices for the *B*-site cations a layered ordering of the *A*-site cations can be obtained (Fig. 1). The layered ordering is stabilized by the presence of a highly charged d^0 cation on one of the *B*-sites [1]. Neutron diffraction studies have revealed that several compounds of this structure type adopt non-centrosymmetric unit cells as a result of the cation ordering in conjunction with octahedral tilting [2]. In addition to this complex scheme of cation ordering, long range nanoscale compositional modulation has been discovered in one member of this group. A recent transmission electron microscopy (TEM) study of NaLaMgWO$_6$ found that the structure consists of alternating stripes, each approximately 24 Å wide. EELS measurements show that the stripe formation is associated with a compositional modulation [3].

The magnetic properties of these systems are also of interest. NaLaMnWO$_6$, NaNdMnWO$_6$ and NaTbMnWO$_6$ have been shown to order antiferromagnetically (AF) at low temperatures [2]. The magnetic structures have been determined by neutron diffraction [4]. In NaLaMnWO$_6$ the Mn^{2+} ions order into a simple commensurate structure driven by antiferromagnetic Mn–O–W–O–Mn superexchange interactions similar to related A_2MnWO$_6$ perovskites. When Nd is substituted for La, the Mn^{2+} and Nd^{3+} magnetic sub-lattices order simultaneously into an incommensurate structure. NaTbMnWO$_6$ was found to pass through two magnetic phase transitions upon cooling. First, both magnetic sub-lattices order into a structure requiring two propagation vectors to describe it, one commensurate and one incommensurate. Upon further cooling the incommensurate component disappears and the structure is described solely by the commensurate vector.

The three compounds discussed above clearly illustrate the importance of magnetic coupling between the two sub-lattices. However, the details of this coupling are not fully understood. The goal of this work is two-fold. First of all, to synthesize and characterize the remaining members of the Na*Ln***Mn**WO$_6$ series, in order to elucidate the trends in magnetic behavior as the radius of the lanthanide ion decreases and the filling of the 4*f* orbitals increases. Secondly, by synthesizing and characterizing the Na*Ln***Mg**WO$_6$ series the magnetic behavior of the *Ln*$^{3+}$ sub-lattice in the absence of magnetic coupling with other ions can be evaluated. Together these studies allow us to better understand the coupling between Mn^{2+} and *Ln*$^{3+}$ sub-lattices. Toward this goal we have therefore prepared 14 new compounds and characterized

* Corresponding author.
E-mail address: gking@chemistry.ohio-state.edu (G. King).

0022-4596/$ - see front matter © 2009 Elsevier Inc. All rights reserved.
doi:10.1016/j.jssc.2009.02.033

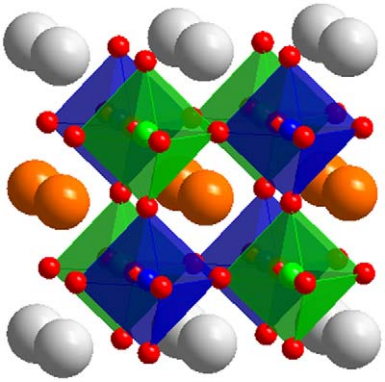

Fig. 1. A depiction of the undistorted $AA'BB'O_6$ perovskite structure with ordering of both cation sub-lattices. Small green (white) and small blue (black) spheres are the *B*-site cations. Large light gray and large orange (dark gray) spheres represent the *A*-site cations. Small red (gray) spheres are the oxygen atoms. (For interpretation of the references to color in this figure legend, the reader is referred to the webversion of this article.)

them by X-ray powder diffraction (XRD) and magnetic susceptibility measurements. These can be classified into two series, the Na*Ln***Mn**WO_6 series and the Na*Ln***Mg**WO_6 series. Their structural features and magnetic behavior are reported here.

2. Experimental

The ceramic method was used for the preparation of all compounds. The starting materials used were: Na_2CO_3 (Fisher, 99.9%), $MgWO_4$, $MnWO_4$ (Alfa Aesar, 99.9%), CeO_2 (Acros, 99.9%), Pr_6O_{11} (Alfa Aesar, 99.9%), Sm_2O_3 (Cerac, 99.9%), Eu_2O_3 (Alfa Aesar, 99.9%), Gd_2O_3 (Alfa Aesar, 99.99%), Tb_4O_7 (Cerac, 99.9%), Dy_2O_3 (Cerac, 99.9%), Ho_2O_3 (Alfa Aesar, 99.9%). The $MgWO_4$ precursor was prepared from MgO (Allied, 99.9%) and WO_3 (Alfa Aesar, 99.9%) using the ceramic method. All Ln_2O_3 reagents were heated to 900 °C for 6 h prior to use to ensure the removal of any absorbed water. A 2% excess of Na_2CO_3 was used to account for the high temperature volatility of sodium.

The Na*Ln***Mg**WO_6 compounds could be synthesized by heating to temperatures ranging from 900 to 950 °C for 8 h. When $Ln = Ce$ it was necessary to heat under forming gas (95% N_2, 5% H_2) to ensure a +3 oxidation state for the cerium. All other compounds in this series could be synthesized in air.

The Na*Ln***Mn**WO_6 compounds could be synthesized by heating to temperatures ranging from 900 to 1000 °C for 8 h. All of these compounds were synthesized under the flow of forming gas. This was necessary in order to prevent the oxidation of Mn^{2+} to Mn^{3+}. Final annealing temperatures for all compounds are shown in Table 1.

The X-ray diffraction experiments were preformed on a Bruker D8 diffractometer (40 kV, 50 mA, Cu$K\alpha_1$ radiation) equipped with a Braun linear position-sensitive detector and a Ge 111 incident beam monochromator. Scans were taken over a 2θ range of 8°–90° with a step size of 0.014286° and a dwell time of 2 s. Structure refinements were done using the Topas Academic software package [5].

Magnetic susceptibility measurements were carried out on a MPMS XL Quantum Design SQUID magnetometer. The field strength was 1000 Oe. The temperature increment for the Na*Ln***Mn**WO_6 compounds was 1 K for temperatures from 2 to 24 K and 4 K for temperatures from 24 to 300 K. For the Na*Ln***Mg**WO_6 compounds the temperature increment was 1 K for temperatures between 2 and 10 K and 5 K for temperatures between 10 and 200 K, except for $Ln = Sm$ or Eu in which case data was collected up to 300 K using a 10 K interval from 200 to 300 K.

Table 1
The final annealing temperatures, colors, and impurity levels for the samples prepared in this study.

Compound	Annealing temperature (°C)	Color	Impurity level
$NaCeMgWO_6$	950	Dark green	Trace
$NaPrMgWO_6$	950	Light green	None
$NaSmMgWO_6$	900	Off-white	Trace
$NaEuMgWO_6$	900	White	Trace
$NaGdMgWO_6$	950	White	None
$NaTbMgWO_6$	900	Tan	Trace
$NaDyMgWO_6$	900	White	Trace
$NaHoMgWO_6$	900	Pink	Trace
$NaCeMnWO_6$	1000	Brown	None
$NaPrMnWO_6$	900	Green	None
$NaSmMnWO_6$	900	Green	None
$NaGdMnWO_6$	900	Forest green	Small
$NaDyMnWO_6$	900	Green	Small
$NaHoMnWO_6$	950	Yellow-green	Large

3. Results and discussion

3.1. Synthesis

Fourteen new perovskite compounds have been synthesized. One additional composition, $NaEuMnWO_6$, was attempted but could not be made. The inability to form this composition is linked to the tendency of europium to be reduced to the +2 oxidation state when heated under forming gas. The use of forming gas is necessary to prevent oxidation of Mn^{2+} but inevitably leads to reduction of Eu^{3+} to Eu^{2+}. Therefore, this composition could not be obtained.

Many of the samples contained a small impurity of Na_2WO_4 after the initial synthesis that did not diminish with additional grinding and heating. This impurity was removed by washing the samples with water. A Na_2WO_4 impurity could be caused by the presence of a compositional modulation, similar to what has been proposed for $NaLaMgWO_6$ as described in Ref. [3]. If something similar is occurring in these samples there would be regions of the sample deficient in Na^+ which are compensated by an Ln^{3+} excess, with the Na^+ deficiency being three times that of the Ln^{3+} excess. This would explain why a Na rich impurity phase is observed.

After washing, most samples appeared to be phase pure or nearly so according to XRD. Within the Na*Ln*$MgWO_6$ series those with $Ln = Pr$ and Gd appear to be completely phase pure within the detection limits of XRD. The other six samples have a very weak peak at either 28.6° (Sm and Eu) or 29.2° 2θ (Ce, Tb, Dy, Ho) that is not accounted for by the perovskite phase. Since only one peak of these impurity phases is noticeable the composition of this secondary phase could not be determined.

The three members of the Na*Ln*$MnWO_6$ series with the largest *Ln* (Ce, Pr, and Sm) were all phase pure according to XRD. The other three samples (Gd, Dy, Ho) each contained secondary phases. The impurity levels in the samples with $Ln = Gd$ and Dy were small while the amount of impurity in the sample with $Ln = Ho$ is rather large. These secondary phases could not be washed away and did not diminish with additional grinding and heating. The reason why these samples could not be made in pure form may be related to the small tolerance factors of these compositions. As the tolerance factor is decreased the perovskite phase eventually becomes destabilized and other phases become competitive. This would explain why the relative amount of the impurity phase increases as smaller lanthanides are used.

A previous paper has reported unsuccessfully attempting to synthesize $NaYMnWO_6$ [2]. Since Y^{3+} and Ho^{3+} very nearly have the same ionic radii this is further evidence that the tolerance factor of $NaHoMnWO_6$ ($\tau = 0.899$) is at the lower limit of the stability range.

3.2. Structural characterization

XRD was used to perform a preliminary structural characterization of these materials. Rietveld refinements were carried out to confirm the structures and extract the lattice parameters. The possible space groups that can be adopted by perovskites as a result of these two types of cation ordering in combination with tilting of the BO_6 octahedra have been previously determined by group theory [1]. The undistorted and fully ordered $AA'BB'O_6$ perovskite has tetragonal symmetry and belongs to space group $P4/nmm$. The symmetry can be lowered by octahedral tilting. All compounds examined in this study were found to have unit cell parameters that are either metrically tetragonal or monoclinic. There are two possible types of monoclinic unit cells for this class of perovskites. The unit cell dimensions can either be $2a_p \times 2a_p \times 2a_p$ or $\sqrt{2}a_p \times \sqrt{2}a_p \times 2a_p$ (where a_p is the cell edge of the basic ABO_3 cubic perovskite). The peak splitting observed for all of the monoclinic perovskites in this study shows them to fall into the latter category. This is most clearly seen by looking at the pseudo-cubic $(\frac{111}{222})$ reflection, as indexed on a cubic a_p cell. As seen in Fig. 2 this peak is split into the monoclinic (011), $(\bar{1}01)$ and (101) reflections which is consistent with a $\sqrt{2}a_p \times \sqrt{2}a_p \times 2a_p$ cell. In contrast, a $2a_p \times 2a_p \times 2a_p$ cell only allows for two reflections at this position.

The observation of a $\sqrt{2}a_p \times \sqrt{2}a_p \times 2a_p$ cell limits the possible space groups for these compounds to either $P2_1/m$ (Glazer tilt system $a^-a^-c^0$) or $P2_1$ (Glazer tilt system $a^-a^-c^+$). These two space groups have the same reflection conditions and can only be differentiated by peak intensities. Since XRD is not very sensitive to oxygen positions when heavy elements are present, neutron diffraction would be needed to definitively assign which space group these belong to and to provide reliable positions for the oxygen atoms. It should also be noted that some of these compounds may also have long range compositional modulations [2] or octahedral tilt twinning [6]. It has been shown that XRD is not sensitive to these structural features [3]. Neutron diffraction and electron microscopy studies that will provide a more detailed picture of the crystal structure are currently in progress.

XRD is highly sensitive to the presence of cation ordering. The presence of cation ordering could be determined by the presence of supercell reflections. Layered A-site cation ordering is revealed by the presence of pseudocubic $(00\frac{1}{2})$ and $(10\frac{1}{2})$ reflections. Rock-salt ordering of the B-site cations is indicated by pseudocubic $(\frac{111}{222})$ reflections. These supercell reflections are present in the XRD patterns of all samples indicating that all compounds reported in this study have ordering on both the cation sub-lattices. The refinements have indicated the degree of cation ordering in these compounds is complete or very nearly so in all cases. Fig. 3 shows two examples of XRD patterns of these compounds.

Within each of the two series the compounds with larger lanthanides (Ce and Pr) were found to be metrically tetragonal. Interestingly, the La members of each series have been previously reported to be monoclinic, although they are still pseudo-tetragonal [1,2]. The compounds with smaller lanthanides (Sm, Eu, Gd, Tb, Dy, Ho) are monoclinic. Full XRD patterns of all compounds and additional details of the refinements are given in the supporting information.

Now that the unit cells of a large number of these compounds have been obtained it is possible to observe the trends in the lattice parameters as the lanthanide is varied. Fig. 4 shows plots of the lattice parameters vs. lanthanide radius for both series. For the Na*Ln***Mn**WO_6 series the a and b parameters decrease steadily while the metric symmetry remains tetragonal. Once the symmetry switches to monoclinic the b parameter increases and then remains approximately constant as the lanthanide continues to become smaller. Meanwhile, the a parameter decreases rapidly. The c parameter as well as the volume decreases steadily as the lanthanide size decreases, with two small anomalies for the c parameter. The Na*Ln***Mg**WO_6 series shows similar trends. As the lanthanide size is decreased a and b decrease together until the symmetry becomes monoclinic after which b stays nearly constant and a decreases rapidly. A small anomaly in c and the volume occurs at Nd where the metric symmetry switches. The lattice parameters of all compounds are given in Table 2.

Octahedral tilting in perovskites is usually considered a result of the A-site cations being too small to fill the cubo-octahedral

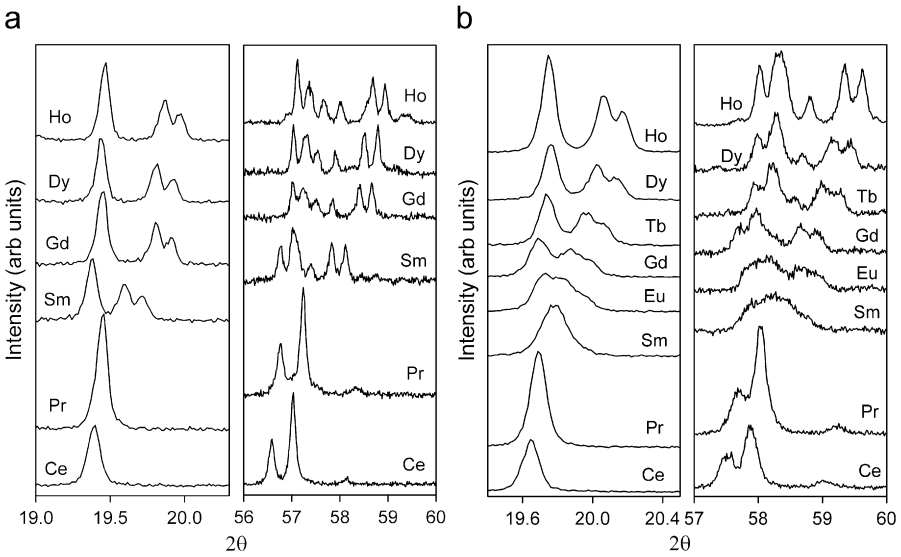

Fig. 2. Selected regions of the powder XRD patterns for (a) Na*Ln***Mn**WO_6 compounds and (b) Na*Ln***Mg**WO_6 compounds. The left sides of the figures show the evolution of the pseudo-cubic $(\frac{1}{2}\frac{1}{2}\frac{1}{2})$ peak and the right side shows the evolution of the pseudo-cubic (112) peak.

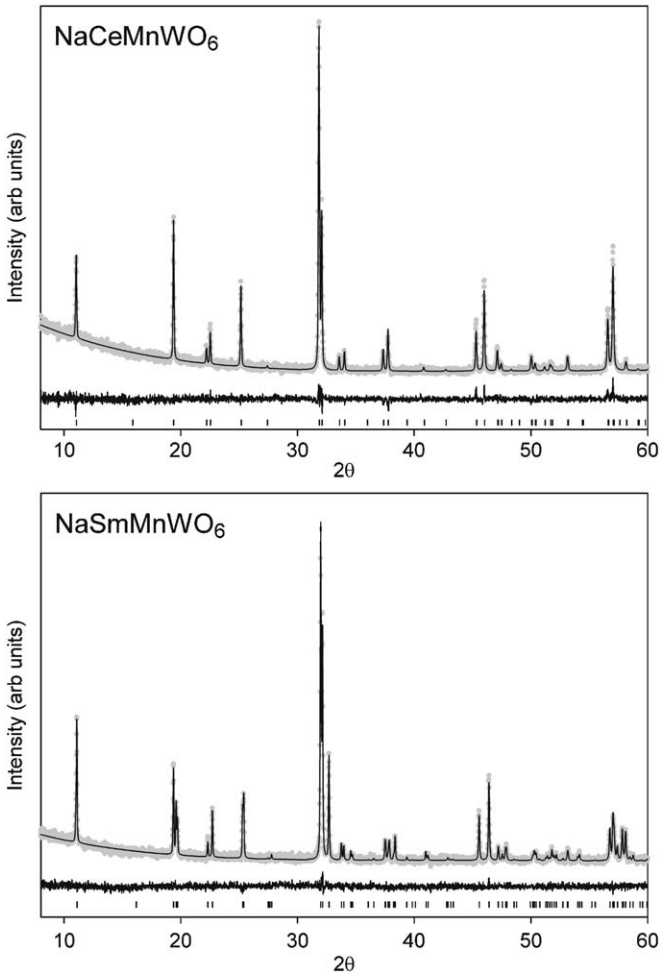

Fig. 3. The X-ray powder diffraction patterns of $NaCeMnWO_6$, which exhibits a metrically tetragonal unit cell, and $NaSmMnWO_6$, which exhibits a monoclinic unit cell. The experimental pattern (gray circles), calculated (black solid line), and difference (beneath) are shown. Tick marks show allowed *h k l* reflections.

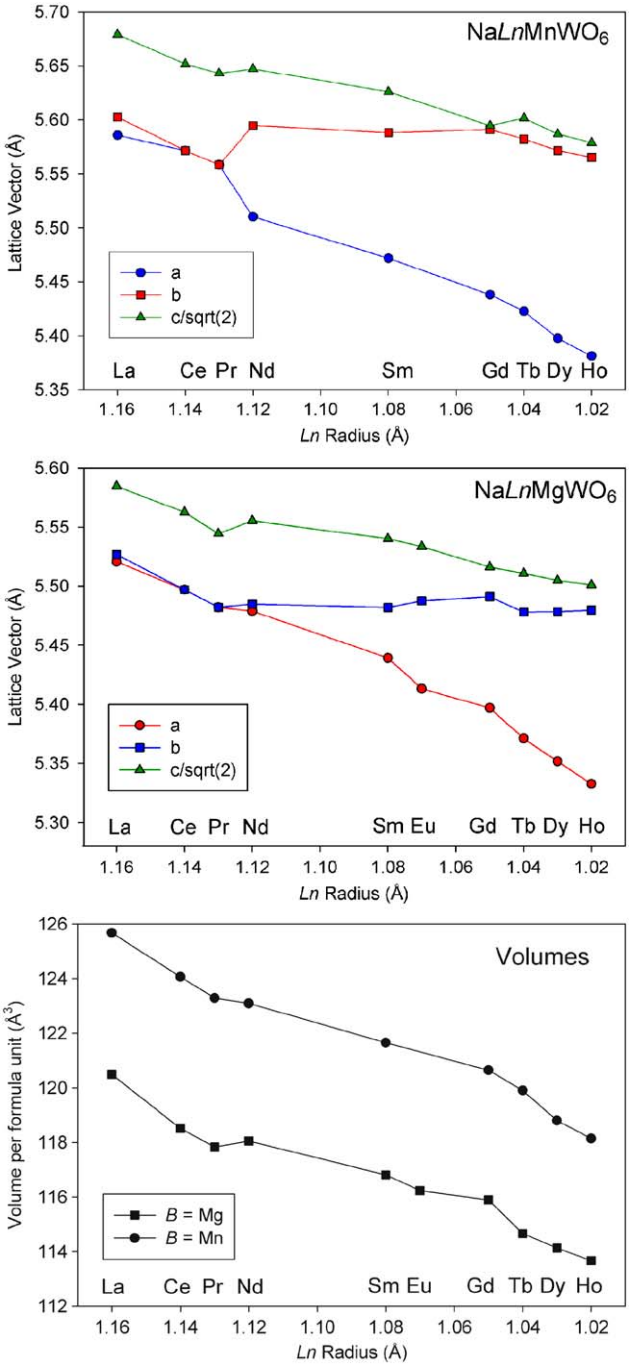

Fig. 4. Plots of lattice parameters vs. 8-coordinate lanthanide radius for both series of compounds using data from this study and previous work [1,2]. The *c* parameter is divided by $\sqrt{2}$ to make it a comparable size.

cavity formed by the BO_3 network. In $AA'BB'O_6$ perovskites deviations from tetragonal symmetry result from octahedral tilting. The tolerance factors for all of these compounds are sufficiently small that octahedral tilting is expected. The largest tolerance factor is for $NaCeMgWO_6$ ($\tau = 0.948$). Normally a tolerance factor this small would necessitate some octahedral tilting [7]. In fact, tetragonal lattice parameters can be observed for a tolerance factor as low as 0.924 for $NaPrMnWO_6$. The program SPuDS [7,8] was used to calculate the expected space groups and lattice parameters based on bond valence optimization for all compounds, assuming a random distribution of the *A*-site cations. The results show that tilting is highly favorable for all compositions. The tilt system $a^-a^-c^+$ is predicted to be the most stable. $P2_1$ space group symmetry is expected for $a^-a^-c^+$ tilting in combination with both types of cation ordering [1]. This suggests that although some of these compounds are metrically tetragonal, the true symmetry is probably lower. Distortions from the ideal perovskite structure in which the lattice parameters remain essentially equivalent have been known to occur in other perovskite systems when the octahedra distort in addition to rotating [9,10].

It should also be noted that the tetragonal to monoclinic transition does not occur at the same tolerance factor in both of the series. Since Mg^{2+} is smaller than Mn^{2+} the tolerance factors for the Mg containing compounds are larger than the Mn containing analogues. The largest of the Na*Ln*$MnWO_6$ series, NaCe**Mn**WO_6 ($\tau = 0.926$), is metrically tetragonal. This tolerance factor lies between that of $NaTbMgWO_6$ and $NaDyMgWO_6$ which are both monoclinic. The Na*Ln***Mg**WO_6 series has its first visible monoclinic distortion at $\tau = 0.940$ while the Na*Ln***Mn**WO_6 series does not show a monoclinic distortion of the unit cell until $\tau = 0.918$. However, both series undergo the tetragonal to monoclinic transition between Pr and Nd. It appears as though the size mismatch between the two types of *A*-site cations plays an important role in determining the metric symmetry.

Table 2
Lattice parameters and tolerance factors of Na*Ln*BWO$_6$ compounds prepared in this study and other studies [1,2].

Compound	a (Å)	b (Å)	c (Å)	β (deg)	V/Z (Å^3)	τ
NaLaMgWO$_6$[1,a]	5.5277(1)	5.5266(1)	7.8977(1)	90.136(1)	120.48(1)	0.952
NaCeMgWO$_6$	5.4970(1)		7.8667(3)		118.51(1)	0.948
NaPrMgWO$_6$	5.4822(1)		7.8411(3)		117.83(1)	0.946
NaNdMgWO$_6$[2]	5.4789(2)	5.4848(2)	7.8566(3)	90.16(0)	118.05(1)	0.940
NaSmMgWO$_6$	5.4392(3)	5.4820(3)	7.8349(5)	90.202(6)	116.81(2)	0.937
NaEuMgWO$_6$	5.4133(3)	5.4876(3)	7.8255(4)	90.297(3)	116.23(2)	0.934
NaGdMgWO$_6$	5.3970(3)	5.4911(3)	7.8215(4)	90.325(3)	115.90(2)	0.933
NaTbMgWO$_6$	5.3712(2)	5.4781(2)	7.7935(3)	90.323(2)	114.66(1)	0.927
NaDyMgWO$_6$	5.3517(2)	5.4785(2)	7.7852(3)	90.341(2)	114.13(1)	0.922
NaHoMgWO$_6$	5.3326(1)	5.4796(1)	7.7798(1)	90.347(1)	113.67(1)	0.921
NaLaMnWO$_6$[2]	5.5857(1)	5.6026(1)	8.0313(1)	90.22(0)	125.67(1)	0.930
NaCeMnWO$_6$	5.5716(1)		7.9927(2)		124.06(1)	0.926
NaPrMnWO$_6$	5.5583(1)		7.9803(2)		123.28(1)	0.924
NaNdMnWO$_6$[2]	5.5101(1)	5.5948(1)	7.9861(1)	90.36(0)	123.09(1)	0.918
NaSmMnWO$_6$	5.4719(1)	5.5883(2)	7.9564(2)	90.367(1)	121.65(1)	0.915
NaGdMnWO$_6$	5.4382(2)	5.5912(2)	7.9352(3)	90.346(2)	120.64(1)	0.911
NaTbMnWO$_6$[2]	5.4228(1)	5.5822(1)	7.9220(1)	89.65(0)	119.90(1)	0.906
NaDyMnWO$_6$	5.3977(1)	5.5716(1)	7.9008(2)	90.358(1)	118.80(1)	0.900
NaHoMnWO$_6$	5.3814(2)	5.5653(2)	7.8896(2)	90.327(2)	118.14(2)	0.899

Tolerance factors were calculated from bond valence parameters using the program SPuDS [7,8]. The tolerance factor is a measure of how well the A-site cation fits within the cubo-octahedral cavity formed between eight BO_6 units in an undistorted perovskite. It is defined as $\tau = (R_A+R_X)/\sqrt{2}(R_B+R_X)$, where R_A, R_B, and R_X, are the ionic radii of the A-cation, B-cation, and anion, respectively. A τ of 1 represents a perfect fit, while a τ of less than 1 means that the A-site cation is too small for the cavity.

[a] This compound was reported in a $2a_p \times 2a_p \times 2a_p$ unit cell. The lattice parameters have been changed to a $\sqrt{2}a_p \times \sqrt{2}a_p \times 2a_p$ unit cell to facilitate comparison.

3.3. Magnetic properties

All of the compounds were magnetically characterized by susceptibility vs. temperature measurements. The compound NaNdMgWO$_6$, which was reported previously but not magnetically characterized [2], was also studied since it provides a basis of comparison for NaNdMnWO$_6$ whose magnetic structure was determined in a related study [4]. Curie–Weiss plots were constructed for all samples to determine the magnetic moment and Weiss constant. For the Na*Ln***Mg**WO$_6$ series the temperature range of 10–200 K was used to make these plots while for the Na*Ln***Mn**WO$_6$ series the temperature range of 40–300 K was used. NaSmMgWO$_6$ and NaEuMgWO$_6$ do not display Curie–Weiss behavior and therefore these parameters could not be obtained for these two compounds. The linear fit to the data for the Curie–Weiss plots was excellent in almost all cases except for NaCeMgWO$_6$ and NaNdMgWO$_6$ which have very minor deviations from linearity. The measured and expected moments were generally in good agreement. The measured moments were in all cases smaller than the theoretical. The difference in most cases was about 5–10%. The observed moments for most of the lanthanides are slightly smaller than the theoretical $g(J(J+1))^{1/2}$ values [11].

The Na*Ln***Mn**WO$_6$ compounds were investigated in hopes of finding more compounds with multiple magnetic phase transitions, similar to what has been reported for NaTbMnWO$_6$ [2,4]. All six members of this series were found to order AF at low temperatures. Plots of magnetic susceptibility vs. temperature for Na*Ln***Mn**WO$_6$ compounds are shown in Fig. 5. Table 3 shows the magnetic parameters for compounds from the Na*Ln***Mn**WO$_6$ series (including previously published results). The Néel temperatures (T_N) ranged from 10 to 13 K. The Weiss constants show a general trend of decreasing as the size of the lanthanide is deceased, with NaSmMnWO$_6$ as an exception. The decreasing

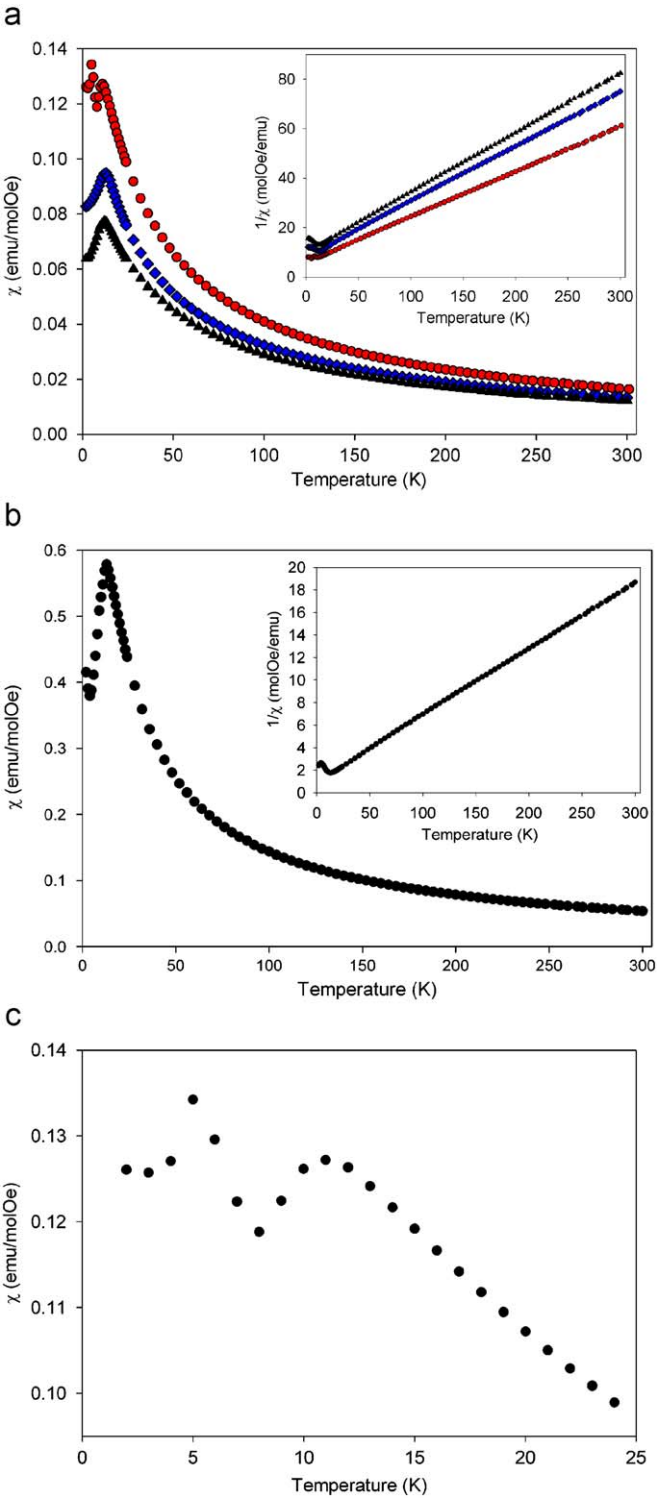

Fig. 5. Plots of magnetic susceptibility vs. temperature for Na*Ln*MnWO$_6$ compounds with inverse susceptibility vs. temperature plots shown as inserts. (a) Red circles are Ln = Pr, blue diamonds are Ln = Ce, and black triangles are Ln = Sm, (b) Ln = Dy and (c) a low temperature magnification of the NaPrMnWO$_6$ curve. (For interpretation of the references to color in this figure legend, the reader is referred to the webversion of this article.)

Weiss constants can be rationalized in terms of weaker superexchange resulting from octahedral tilting. As the octahedra tilt the Mn–O–W bond angles deviate from 180° which weakens orbital overlap.

Table 3
Magnetic data on Na*Ln*BWO_6 compounds from this study and from Ref. [2].

Compound	C (emu K/mol Oe)	Θ (K)	μ_{eff}/μ_B	μ_{theory}/μ_B	Transition temperatures (K)
$NaCeMgWO_6$	0.608(2)	−14.1(2)	2.21(2)	2.54	None
$NaPrMgWO_6$	1.28(1)	−35.8(1)	3.20(1)	3.58	None
$NaNdMgWO_6$	1.40(2)	−32.3(3)	3.34(2)	3.62	None
$NaGdMgWO_6$	4.757(1)	−1.63(1)	6.17(1)	7.94	None
$NaTbMgWO_6$	10.6(2)	−4.20(2)	9.21(2)	9.72	None
$NaDyMgWO_6$	13.0(2)	−3.68(2)	10.2(2)	10.63	None
$NaHoMgWO_6$	12.51(1)	−8.26(2)	10.0(1)	10.60	None
$NaLaMnWO_6^2$	4.369(3)	−42.25(6)	5.911(3)	5.92	10
$NaCeMnWO_6$	4.54(2)	−40.02(3)	6.02(2)	6.44	13
$NaPrMnWO_6$	5.49(2)	−34.02(2)	6.63(1)	6.92	11, 8, 5
$NaNdMnWO_6^2$	5.938(2)	−35.43(5)	6.891(2)	6.94	11
$NaSmMnWO_6$	4.16(1)	−43.06(4)	5.77(1)	5.98	12, 3
$NaGdMnWO_6$	8.58(3)	−27.38(2)	8.28(3)	9.90	13
$NaTbMnWO_6^2$	16.52(1)	−27.29(1)	11.49(1)	11.38	15, 9
$NaDyMnWO_6$	17.1(2)	−19.09(2)	11.7(2)	12.17	13, 4
$NaHoMnWO_6$	17.3(2)	−19.47(3)	11.8(2)	12.14	11

The Curie constant (C), Weiss constant (Θ), effect magnetic moment, theoretical magnetic moment [11], and observed transition temperatures are given.

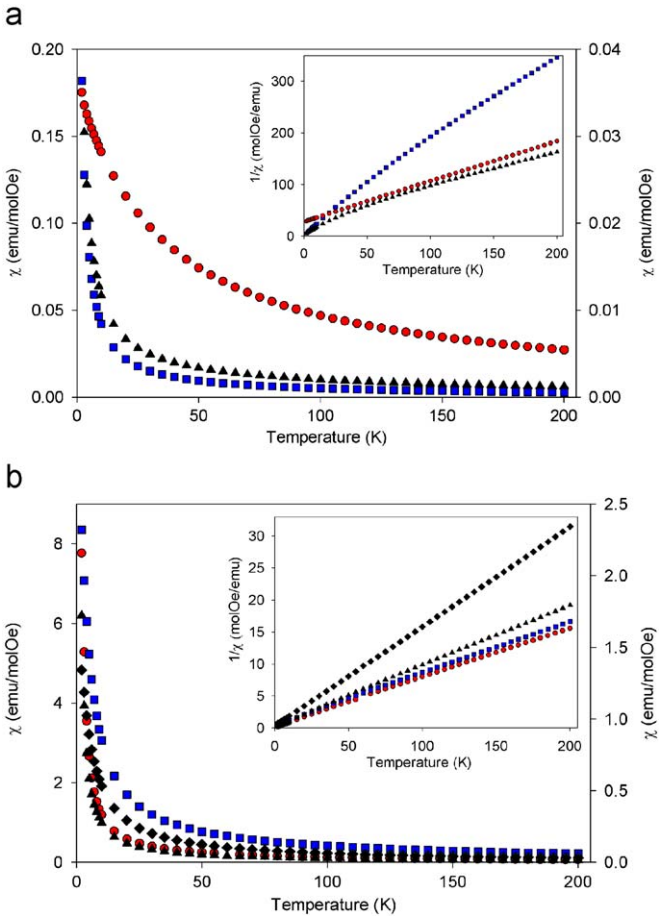

Fig. 6. Plots of magnetic susceptibility vs. temperature for Na*Ln*$MgWO_6$ compounds with inverse susceptibility vs. temperature plots shown as inserts. (a) Blue squares are Ln = Ce (left y-axis), black triangles are Ln = Nd (left y-axis), and red circles are Ln = Pr (right y-axis), (b) red circles are Ln = Dy (left y-axis), black triangles are Ln = Tb (left y-axis), blue squares are Ln = Ho (right y-axis), and green diamonds are Ln = Gd (right y-axis). (For interpretation of the references to color in this figure legend, the reader is referred to the webversion of this article.)

The compound $NaCeMnWO_6$ shows a simple susceptibility curve with a single AF transition at 13 K where the Mn^{2+} and Ce^{3+} appear to order simultaneously. $NaSmMnWO_6$ passes through an AF transition at 12 K. The susceptibility shows a slight upturn at 3 K. It is worth noting that the fit to the Curie–Weiss plot for this sample shows no deviation from linearity. Since Mn^{2+} is the dominant magnetic species it would be expected that the curve should be close to linear, however, the non-Curie Weiss behavior of Sm^{+3} would be expected to introduce some deviation to the linearity, but none is observed. $NaDyMnWO_6$ has an AF transition at 13 K and shows a clear second transition at 4 K where the susceptibility begins to increase rapidly. The upturns in the susceptibilities are most likely the result of a second phase transition. A second magnetic phase transition accompanied by an upturn in the susceptibility has been confirmed by neutron diffraction for $NaTbMnWO_6$ [4] so it is reasonable to expect it could occur for similar compounds with different lanthanides. However, it is difficult to completely rule out the possibility that a small amount of a paramagnetic impurity could be causing this effect.

The $NaGdMnWO_6$ and $NaHoMnWO_6$ samples show magnetic transitions at 13 and 11 K, respectively. The susceptibilities continue to increase below these temperatures, although no longer as quickly as they should if they were Curie–Weiss paramagnets. Therefore, these transitions should still be considered AF in nature. This continued increase is most likely due the presence of paramagnetic impurities in these samples since XRD has revealed that both samples have significant amounts of a secondary phase.

The $NaPrMnWO_6$ sample has the most interesting magnetic behavior of all the samples studied. It appears to have at least three closely spaced magnetic phase transitions (see Fig. 5c). It first passes through a paramagnetic to AF transition at 11 K. At 8 K the susceptibility starts to rise once again as has been seen for several other compounds within this series. But then at 5 K the susceptibility begins to decrease sharply. The XRD analysis has indicated that this sample is phase pure. The same behavior was reproduced on a separate sample. The nature of this behavior is still quite mysterious and neutron diffraction experiments will be needed to unravel the nature of this complex ordering.

The compounds of the Na*Ln***Mg**WO_6 series were studied to gain an understanding of how the layers of magnetic lanthanides would order. All nine members of this series show no indications of any magnetic order, remaining paramagnetic down to a temperature of 2 K. This behavior reveals that the exchange interaction between the lanthanide cations is very weak. It can be concluded that in all of the Na*Ln***Mn**WO_6 compounds superexchange between the Mn^{2+} ions provides the driving force for ordering and that the ordering of the Mn^{2+} ions induces the ordering of the Ln^{3+} ions.

With the exception of the Sm and Eu containing compounds, all of the other seven members of the Na*Ln***Mg**WO_6 series show Curie-Weiss behavior down to 2 K. Curie–Weiss plots are shown in Fig. 6 and the parameters extracted from these plots are given in Table 3. The Weiss constants of all these samples were negative indicating that the exchange interaction is AF in nature. The magnitudes of the Weiss constants were generally small (−1.6 to −14.1 K) indicating the exchange interactions are quite weak, which is consistent with the fact that the moments do not order. The exceptions were the compounds with Ln = Pr and Nd. These had larger Weiss constants (−35.8 and −32.3 K, respectively) that were comparable to those of the Na*Ln***Mn**WO_6 series, although perhaps surprisingly there was still no indication of ordering.

The compounds $NaSmMgWO_6$ and $NaEuMgWO_6$ show van Vleck magnetic behavior (see Fig. 7). Both the Sm^{3+} and Eu^{3+} ions have low lying excited states that are thermally populated at ambient temperatures. This trait gives them

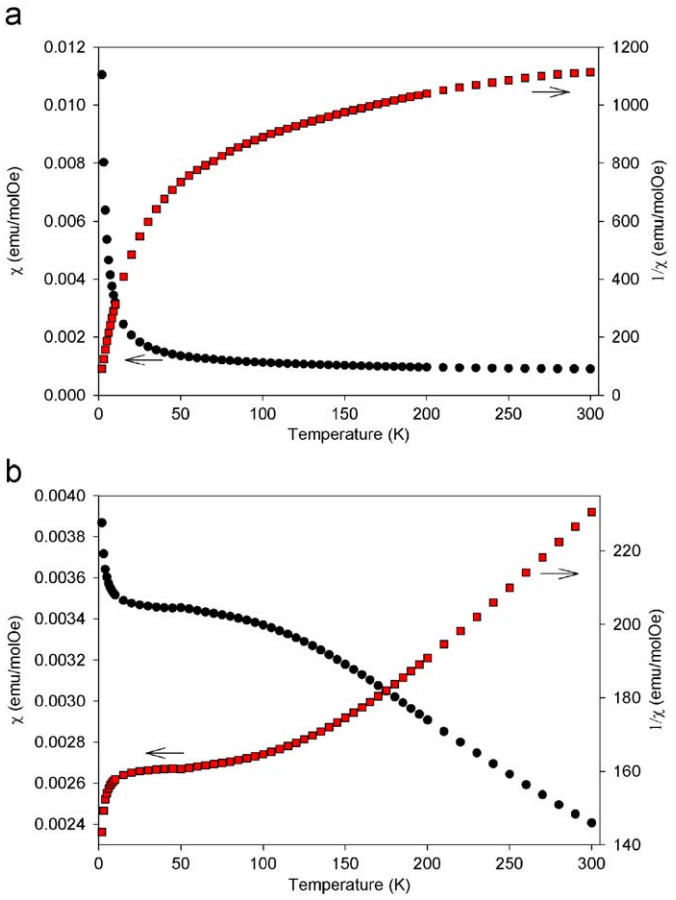

Fig. 7. Plots of magnetic susceptibility vs. temperature (black circles) and inverse susceptibility vs. temperature (red squares) for (a) $NaSmMgWO_6$ and (b) $NaEuMgWO_6$. (For interpretation of the references to color in this figure legend, the reader is referred to the webversion of this article.)

additional temperature dependence. The $^6H_{5/2}$ ground state of Sm^{3+} has a moment of 0.84 μ_B but the moment is typically about 1.5 μ_B at room temperature due to thermal population of the $^6H_{7/2}$ first excited state [11,12]. The Eu^{3+} ion has a non-magnetic ground state but due to thermal population of the first two excited states it has an effective moment of about 3.4 μ_B at ambient temperatures [11,13]. The susceptibility of $NaSmMgWO_6$ increases steadily as the temperature is lowered and the shape of the curve is similar to what has been reported for other Sm^{3+} containing compounds [12,14]. The susceptibility of $NaEuMgWO_6$ slowly increases as the temperature is lowered until around 75 K where it levels off. At this point it loses its temperature dependence since the thermal population of excited states has become negligible. The moment does not drop to zero at these temperatures because there is still an effective moment due to coupling of the ground and first excited state through the Zeeman perturbation. The upturn in the susceptibility starting around 10 K is due to the presence of a paramagnetic impurity, possibly a trace quantity of Eu^{2+}. Since the moment due to Eu^{3+} is so low at these temperatures even a very small quantity of a paramagnetic species would still produce a noticeable effect. The shape of the susceptibility curve of $NaEuMgWO_6$ is similar to theoretical predictions and what has been observed for several other Eu^{3+} containing compounds [12,13,15].

4. Conclusions

Fourteen new $NaLnBWO_6$ perovskite compounds have been prepared. All of the compounds display a rock salt ordering of two different *B*-site cations and a layered ordering of two different *A*-site cations. For larger *Ln* these samples have metrically tetragonal symmetry. When smaller *Ln* are used they adopt monoclinic symmetry. It appears as though the difference in the size of the two *A*-site cations plays an important role in determining the metric symmetry. The lower limit for the tolerance factor appears to be approximately 0.90. For tolerance factors below this it is not possible to obtain phase pure perovskites.

Magnetic susceptibility measurements have found that all compounds of the $NaLn\mathbf{Mn}WO_6$ series order antiferromagnetically at temperatures between 10 and 13 K. The compounds with *Ln* = Sm and Dy, show indications of a possible second magnetic phase transition at lower temperatures. The compound $NaPrMnWO_6$ was found to undergo at least three closely spaced magnetic phase transitions. This behavior is highly unusually and warrants further study. All members of the $NaLn\mathbf{Mg}WO_6$ series were found to remain paramagnetic down to 2 K. This indicates that in the $NaLn\mathbf{Mn}WO_6$ compounds the magnetic ordering of the lanthanides is induced by the ordering of the Mn^{2+} sub-lattice.

Supporting information

The full X-ray powder diffraction patterns of all compounds, including refinements of those patterns, are given in the supporting information.

Acknowledgments

Financial support from the NSF through a Materials World Network grant (MWN-0603128) and the NSF funded Center for the Design of Materials (CHE-0434567) is gratefully acknowledged.

Appendix A. Supplementary material

Supplementary data associated with this article can be found in the online version at 10.1016/j.jssc.2009.02.033.

References

[1] M.C. Knapp, P.M. Woodward, J. Solid State Chem. 179 (2006) 1076.
[2] G. King, S. Thimmaiah, A. Dwivedi, P.M. Woodward, Chem. Mater. 19 (2007) 6451.
[3] S. Garcia-Martin, E. Urones-Garrote, M.C. Knapp, G. King, P.M. Woodward, J. Am. Chem. Soc. 130 (2008) 15028.
[4] G. King, A.S. Wills, P.M. Woodward, Phys. Rev. B, in press.
[5] Topas Academic, General Profile and Structure Analysis Software for Powder Diffraction Data; Bruker AXS: Karlsruhe, Germany, 2004.
[6] B.S. Guiton, H. Wu, P.K. Davies, Chem. Mater. 20 (2008) 2860.
[7] M.W. Lufaso, P.W. Barnes, P.M. Woodward, Acta Cryst. B 62 (2006) 397.
[8] M.W. Lufaso, P.M. Woodward, Acta Cryst. B 57 (2001) 725.
[9] J.-S. Zhou, J.B. Goodenough, Phys. Rev. Lett. 94 (2005) 065501.
[10] P.W. Barnes, M.W. Lufaso, P.M. Woodward, Acta Cryst. B 62 (2006) 384.
[11] N. Spaldin, Magnetic Materials, Cambridge University Press, Cambridge, 2003.
[12] K. Koteswara Rao, M. Vihal, D. Ravinder, J. Magn. Magn. Mater. 253 (2002) 65.
[13] L. Thompson, J. Legendziewicz, J. Cybinska, Li Pan, W. Brennessel, J. Alloys Compd. 341 (2002) 312.
[14] S.J. Mugavero III, M.D. Smith, H.-C. Zur Loye, J. Solid State Chem. 178 (2005) 200.
[15] T. Aitasalo, J. Holsa, M. Lastusaari, J. Legendziewicz, L. Lehto, J. Linden, M. Marysko, J. Alloys Compd. 380 (2004) 296.